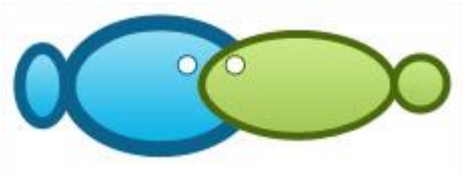

The potential of fish scale application as photothermal raw material in seawater desalination

[1,2]Dolfie P. Pandara, [2]Kawilarang W. A. Masengi, [1]Gerald H. Tamuntuan, [2]Ping A. Angmalisang, [3]Audy D. Wuntu, [1]Ferdy Ferdy, [1]Maria D. Bobanto, [4]Armstrong F. Sompotan

[1] Faculty of Mathematics and Science, Sam Ratulangi University, Manado, Indonesia; [2] Marine Science Doctoral Study Program, Faculty of Fisheries and Marine Science, Sam Ratulangi University, Manado, Indonesia; [3] Faculty of Mathematics and Science, Sam Ratulangi University, Manado, Indonesia; [4] Faculty of Mathematics and Science, Manado State University. Corresponding author: D. P. Pandara, dpandara_fisika@unsrat.ac.id

Abstract. The challenge of accessing clean and potable water due to the increase in human population, economy, and development, as well as global warming, poses a global concern. Solar-powered seawater desalination using photothermal substances appears as a promising environmentally friendly solution. The development of these materials as decayed aquatic samples is very significant. Indonesia produces various marine wastes in large quantities, including fish scales, and the potential conversion into photothermal materials is analyzed by the characterization of the physical and chemical features. The purpose of this study is to evaluate the physicochemical properties of fish scales using energy dispersive spectroscopy (EDS), X-ray fluorescence (XRF), Fourier transform infrared spectroscopy (FTIR), UV-VIS spectroscopy, X-ray diffraction (XRD) and electron microscopy scanning (SEM). Carbon, oxygen, calcium, and phosphorus served as the primary elements in the waste samples. Characterization of the functional group bonds showed collagen and hydroxyapatite as the main mineral components. These constituents naturally exhibit photothermal phenomena under ultraviolet light irradiation and are also amorphous, with the capacity to increase the crystallinity during pyrolysis. Based on the characterization results, fish scales contain carbon in the mineral collagen and showed the unique transition of the orbitals π to π* carbonyl groups, which has the potential to be converted into photothermal material such as Carbon Nano Tubes (CNTs) or Carbon Nano Dots (CNDs) for seawater desalination processes.
Key Words: CNDs, CNTs, collagen, fishery waste, photoexcitation.

Introduction. The demand for clean and potable water appears increasingly problematic, mainly due to the upsurge in human population, economic development, and global warming (Ullah & Rasul 2019; Chen et al 2018). Approximately 1.6 billion persons are known to reside in water crisis regions (Ni et al 2018). The development of seawater desalination technology could serve as an anticipatory solution to water scarcity. This measure is very significant as the ocean provides an abundant water source alternative (Sharif et al 2019; Li et al 2018). Multi-stage flash distillation (MSF), multiple-effect distillation (MED), and reverse osmosis (RO) are the widely applied desalination techniques around the world (Wang 2018). Both MSF and MED require excess energy consumption for high-temperature conditions and also demonstrate significant environmental impact, due to the greenhouse gases generated (Rahmani et al 2016; Liyanaarachchi et al 2014). RO involves high energy levels, although the residues occur in a salt liquid form capable of degrading the surrounding (Ahmadvand et al 2019). The three processes require a massive centralized infrastructure that severely limits practical applications, particularly in offshore locations, minor villages, remote regions, or lesser islands (Zhang et al 2019a). The development of desalination technology with low-level and renewable energy sources, which is environmentally friendly and costs little, as well as having high productivity and

portability, offers a potential alternative to access to clean water and environmental sustainability.

Solar-powered desalination technology supports low-level and efficient energy utilization (Wilson et al 2020; Ullah & Rasul 2019). Under this circumstance, sunlight is used (Gueymard, 2004) to facilitate seawater evaporation to form environmentally friendly salt crystals (Xia et al 2019; Luo & Wan 2013). The photothermal phase serves as the primary process, where sunlight is absorbed and converted into heat for seawater steam generation (Wang et al 2019; Han et al 2018; Ghasemi et al 2014). This stage is due to photoexcitation of the constituent materials, including plasmonic metals, semiconductors, and carbon-based substances. In carbon-based elements, the lattice vibrations are responsible for the photothermal processes during the absorption and conversion of solar energy into heat (Gao et al 2019). These tremors are due to the relaxation of the excited electrons through electron-phonon coupling that involves the transfer of solar energy into a vibrational mode, leading to the increasing temperature of the carbon samples (Vélez-Cordero & Hernandez-Cordero 2015).

Carbon-based materials demonstrate strong physical and chemical properties that support photothermal application (Han et al 2018). The characteristic orbital structure facilitates electron excitation by irradiation at almost every solar wavelength from 300-2500 nm (Dao & Choi 2018). Transformation into nanostructures and morphology possibly enhances the ability to convert sunlight into heat with high efficiency (Liu et al 2019; Zhang et al 2018; Zhang et al 2016). Several studies have shown that the carbon nanomaterials, including CNTs exhibited a black body-like absorptivity, wide absorption band and high thermal efficiency, suitable for photothermal materials (Xia et al 2019; Xu et al 2019; Zhang et al 2018, 2019a; Jiang et al 2018; Chen et al 2017; Yin et al 2017; Wang et al 2016). These advantages are attributed to the abundance of raw materials in the form of biomass, both from agricultural and aquatic waste.

Fish scales are major marine decays with the potential to pollute the environment and adversely impact human health (Kabir et al 2019; Yadav et al 2019). These substances are biocomposite materials extracted into organic and inorganic components, including chitin, lecithin, guanine and collagen fibers, as well as hydroxyapatite crystals and calcium carbonate, respectively (Yang et al 2020; Silva et al 2019; Rumengan et al 2017; Suo-Lian et al 2017). The scales are possibly transformed into carbonaceous matter using pyrolytic and hydrothermal methods (Sahoo et al 2019; Ilnicka & Lukaszewicz 2018). Activated carbon and fish scale-based biochar have been applied as potential biosorbents in eliminating anionic acid from dye solutions (Achieng et al 2019; Kabir et al 2019), as organic pollutants in waste treatment (Poblete et al 2020), as electrodes in electrochemical energy conversion, fuel cells as well as in supercapacitors (Ilnicka & Lukaszewicz 2018) and also as cathode material in lithium-sulfur batteries (Yang et al 2020). Fish scale-based carbon nanosheets have been employed as catalysts with high electrocatalytic activity in batteries (He et al 2020). CNDs obtained from fish scales by hydrothermal technique, have been used to detect drug molecules in human blood serum or biological imaging applications (Athinarayanan et al 2020; Meng et al 2019, Zhang et al 2019b). Fish scales from various species have been used to manufacture photothermal materials such as CNDs. CNDs also have a fluorescent property that is easy to adjust so that they can be used to increase the efficiency of solar energy conversion in photothermal materials (Hou et al 2019). The conversion of fish scales into CNDs materials for seawater desalination remains a research challenge. In the research, fish scales of parrotfish (*Chlorurus sordidus*) and red snapper (*Lutjanus argentimaculatus*) are used because they contain high chitin yield (Rumengan et al 2017). In certain studies, the processing of fish scales into carbon materials was described as a significant effort to mitigate pollution generated by marine waste. The present research proposes the use of fish scale biomass as an alternative and sustainable raw material to produce eco-friendly photothermal samples. The potential of these aquatic skins, including the CNTs or CNDs from pyrolysis, requires further investigation, using the characterization of the underlying physical and chemical properties. The purpose of this study is to evaluate the crystallinity, chemical composition, presence of collagen, and characteristic morphology of the fish scales.

Material and Method

Sample Preparation. The fish scales were obtained from a local market in Manado, North Sulawesi province, Indonesia. The size and weight of the fish samples are about 3 kg or more with a length of about 50 cm. These samples were used to characterize the physical and chemical properties of parrotfish (*Chlorurus sordidus*) and red snapper (*Lutjanus argentimaculatus*) (Rumengan et al 2017). The scales were washed with running water to remove the remains of meat or dirt. This was followed by heating the samples under sunlight for two days to achieve approximately 11% water content. The resulting materials were then rinsed with distilled water and desiccated in an electric Kirin oven type KBO-90M at 1150C for 6 hours to attain a zero water content. The dried fish scales were mashed with a Miller Fomac FCT-Z100 machine at a rotation rate of 28000 rpm. Figure 1 shows the resulting parrotfish (PF) and red snapper (RS) powder after sieving with a 200 (75 μm) and 100 mesh (125 μm), respectively.

a) PF Scale Powder b) RS Scale Powder

Figure 1. Powder samples of fish scales.
Source: Photos taken by authors

Characterization of fish scales. X-ray diffraction (XRD), Fourier transform infra-red (FTIR), energy dispersive spectroscopy (EDS), X-ray fluorescence (XRF), scanning electron microscopy (SEM), and UV-VIS spectroscopy were employed to characterize the fish scale powder at the Central Laboratory of the State University of Malang, East Java, Indonesia. The organic content on the sample surface was measured using the EDS integrated with the SEM FEI Inspect S50, while the metallic and non-metallic elements were characterized by the PANalytical Brand XRF equipment, minipal 4 type. Chemical bond vibrations in fish scale samples were detected using a Shimadzu Fourier transform infrared spectrophotometer (IR-Prestige-21), produced in transmittance mode in Tokyo, Japan. The FTIR spectra were recorded at wavelengths between 4000 and 400 cm-1 with the samples placed in KBr pellets. Jena Specord 200 plus UV-VIS analytical equipment was used to analyze absorbance, transmittance, and reflectance as a function of wavelength. The UV–VIS parameters applied the absorbance mode between 190.00-1100.00 nm with measurement points of 1.00 nm, a rate of 50.0 nm/s, and an integration time of 0.02 s. The sample crystal structure was characterized by x-ray diffraction, using the Panalytical X'pert-Pro diffractometer developed by Almelo, the Netherland. The XRD patterns were recorded at 2θ angles from 7.01°-69.99° with CuKα radiation (λ = 1.54) and CuKβ (λ = 1.39), at a generator voltage of 40 kV and a current of 35 mA at chamber temperature (25^0C). The morphological characteristics of the fish scales were determined with the SEM FEI Inspect S50 equipment produced in Tokyo, Japan. The SEM images were measured at a voltage of 20 kV with magnifications of 100, 500 and 1000.

Results and Discussion

Elemental and metal composition. Table 1 shows the composition of organic and metallic elements in both types of fish scales. Primary components include carbon (24.48% RS and 34.49% PF) and oxygen (35.88% RS and 33.35% PF), followed by calcium (25.03% RS and 20.28% PF) and phosphorus (11.79% RS and 9.48% PF). Metals identified by EDS analysis below 1.24% were Na, Mg and Fe, although the constituents were insignificant compared to the main components.

Table 1

The composition of organic and metallic elements by EDS analysis (Wt%)

	C	*O*	*Na*	*Mg*	*Fe*	*Ca*	*P*
RS	24.48 ± 0.07	35.88 ± 0.09	1.22 ±0.02	0.75 ± 0.01	0.51 ± 0.03	25.03 ± 0.04	11.79 ± 0.02
PF	34.49 ±1.66	33.35 ± 0.59	0.78 ± 0.10	0.56 ± 0.03	0.86 ± 0.02	20.28 ± 1.61	9.48 ± 0.57

Table 2 shows the metallic and non-metallic compositions of parrotfish and red snapper powder after the XRF analysis. Primary components included calcium (83.79% RS, 83.07 % PF) and phosphorus (14.5% RS, 14.1% PF). Other trace elements detected in lesser amounts of less than 2-3% of the total composition were sulfur, iron, cobalt, manganese, zinc, copper, strontium, erbium, europium, rhenium, and ytterbium. Previous studies suggested the presence of inorganic components, including CaO or calcium oxide (Ikoma et al 2003), and $Ca_{10}(PO_4)_6(OH)_2$ or hydroxyapatite (Silva et al 2019). The EDS results indicated the presence of hydroxyapatite biomaterials containing Ca, P, and O.

Table 2

The elemental composition of metals and non-metals by XRF analysis (%)

	P	*S*	*Ca*	*Fe*	*Co*	*Cu*	*Mn*	*Zn*	*Sr*	*Er*	*Re*	*Yb*
RS	14.5	0.30	83.79	0.10	0.03	0.057	-	0.05	0.93	0.2	0.10	-
PF	14.1	0.41	83.07	0.13	-	0.069	0.11	0.13	1.5	-	0.07	0.37

EDS and XRF analyzes confirmed that fish scales from both the PF and RS types contained the main elements of carbon, oxygen, calcium, and phosphorus. The substantial carbon content showed the potential for the conversion to carbon-based materials, including biochar, activated carbon, or CNT by pyrolysis (Achieng et al 2019; Sahoo et al 2019). The Ca-rich inorganic components tend to improve the pyrolysis process due to the catalytic function at temperatures above 700^0 C (Yuan et al 2019). Based on the EDS and XRF results, the Fe also acted as a catalyst to produce a high degree of graphitization in CNT synthesis (Suriani et al 2013; Sengupta & Jacob 2010). In microwave oven pyrolysis, catalysts, including Fe, played a significant role by increasing the effectiveness of microwave absorption and reducing the activation energy of CNT formation (Liu et al 2019).

Chemical Bond Analysis. Figure 2 shows similar FTIR absorption profiles of both scale samples but varied transmittance intensities. FTIR characterization was used to evaluate and identify the presence of collagen and its chemical composition. Amide is the main functional group of type I collagen. Four absorption bands at 1657, 1557, 1244, and 3311 cm^{-1} corresponded to the organic content in RS and PF. These ranges are associated with four types of amide such as type I amide, type II amide, type III amide, and type A amide, respectively, and are also functional groups of type I collagen (Jafari et al 2020; Ikoma et al 2003). Type I amide was interconnected with the stretching vibration of the C=O bond in the carbonyl group (Santana et al., 2015), while type II amide originated from the interaction between the stretching vibrations or axial deformation of C-N and the bending vibrations or angular deformation of N-H (Torres et al 2008). Type III amide was related

to the bending vibration of the N-H bond (Jafari et al 2020), and the vibrations of C-N as well as N-H bonds in type II amide and type III amide confirmed the presence of a three-helical collagen structure (Santos et al 2009). The absorption of type A amide in the 3311 cm^{-1} bands was connected to the stretching vibration of the N-H peptide bonds in hydrogen, leading to a frequency change (Paul et al 2017). The organic content of fish scales was observed in bands 2378, 2974 and 3512 cm^{-1} that are associated with the C=O in the CO_2 group (Müsellim et al 2018), antisymmetric stretching vibration of the CH_2 molecule (Santana et al 2015; Santos et al 2009) and the stretching vibration of the OH bond (Arykbaev et al 2020). The FTIR spectra confirmed the presence of an inorganic phase, including the hydroxyapatite mineral with the appearance of absorption bands at 1086 and 565 cm^{-1} linked to the vibrational mode of the phosphate ion and also 1451 and 873 cm^{-1} associated with the CO bond vibrations of the carbonate group in the apatite structure (Silva et al 2019; Santos et al 2009; Torres et al 2008; Ikoma et al 2003). Phosphate and amide content, particularly type I, was also detected by Raman spectroscopy (Ghods et al 2020; Arola et al 2018). The FTIR results showed that the fish scales for both RS and PF were the nanocomposites of type I collagen, carbonate ions, and apatite (Silva et al 2019). The collagen and hydroxyapatite content contributed significantly to the high absorbance of the IR spectrum, based on the Lambert-Beer principle (Listiaji & Suparta 2020). These collagen fibers were also believed to influence the synthesis of nitrogen-doped carbon materials (Yang et al 2020).

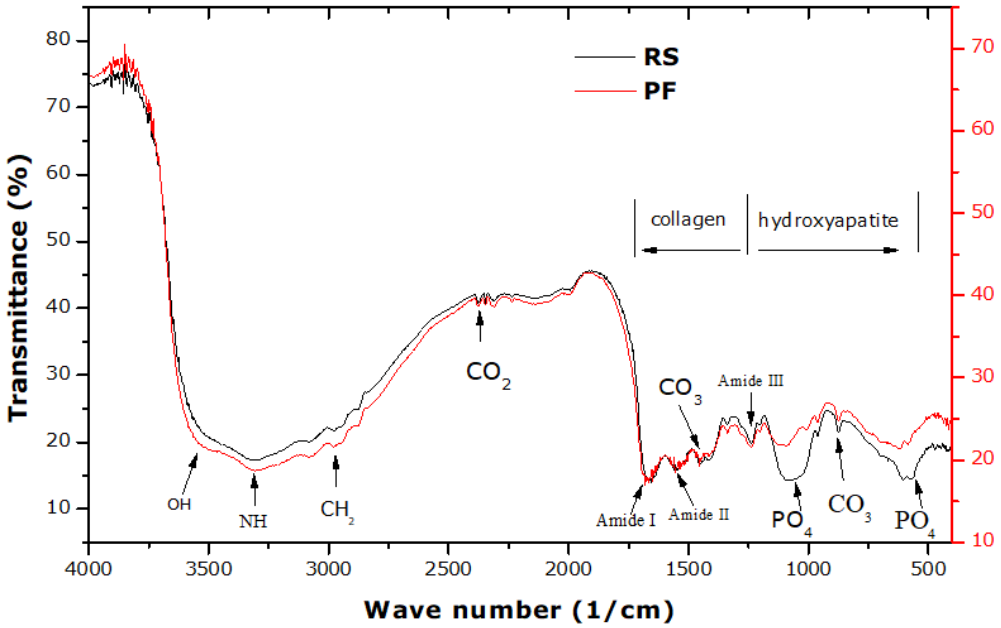

Figure 2. Infrared spectrometer for fish scale residue.
Source: Authors' elaboration

Photoabsorption Analysis. The UV-Vis spectrometer recorded a similar absorbance pattern between the two types of fish scale. Figure 3 shows high absorbance values in the UV wavelength range of 190-300 nm. These results are a characteristic of protein on the fish scales with a maximum absorption peak corresponding to collagen (Gao 2021). The absorbance pattern indicated a higher absorptivity in the parrotfish samples, compared to the red snapper, particularly in the visible area. This indicates that the collagen content in the PF sample is higher than that of the RS sample. The carbonization process by pyrolysis was expected to increase the optical absorptivity because the structure of fish scales is transformed into carbonaceous materials such as CNDs or CNTs, especially for the visible region.

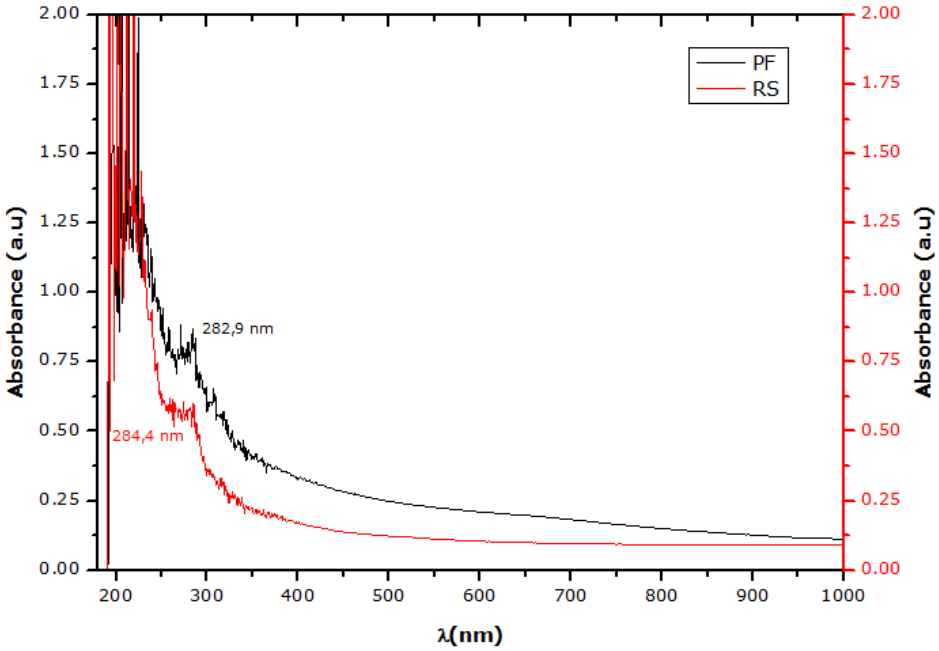

Figure 3. UV-Vis absorbance pattern of fish scales.
Source: Authors' elaboration

The spectral peaks at wavelengths of 282.9 and 284.4 nm were similar to the UV-VIS spectroscopic characteristics investigated on carbon dots from Russian Kraper fish scales, and the unique transition of the orbitals π to π* carbonyl groups are represented at 280 nm (Athinarayanan et al 2020). The carboxyl group is related to the type III amide of the collagen structure (Jafari et al 2020). The unique transition of π to π* orbitals plays a significant role in the photothermal processes (Gao et al 2019; Vélez-Cordero & Hernandez-Cordero 2015). In carbon allotropes, including CNTs and graphene, the number of π conjugated bonds is known to facilitate the electron excitation by irradiating virtually every wavelength of sunlight due to the variations in the π - π* transition. As CNT or graphene is illuminated by the electronic transition in the molecule, a light-absorbing electron is promoted from the ground state or the highest occupied molecular orbital (HOMO) to a higher level or lowest unoccupied molecular orbital (LUMO). The excited electrons tend to relax through electron-phonon coupling, where the absorbed light energy is transferred to the vibrational mode through the atomic lattice, resulting in the temperature increase of the material (Vélez-Cordero & Hernandez-Cordero 2015). These characteristics enhance the electron appearance to resemble black objects, where the carboxyl group of the wastes in one of the allotrophs of the carbon nanomaterial optimizes the photothermal properties for the hot steam generation process. The use of photothermal materials induces localized surface heating and reduces the temperature polarization to obtain a higher thermal efficiency (Han et al 2019). CNTs with organic ligand functional groups are capable of eliminating heavy metals in the wastewater content (Bassyouni et al 2020; Yu et al 2014). Carbon nanomaterials, including fish scale carbon dots, possess natural organic ligands (Zhang et al 2019a). These fish scales are potentially converted into CNTs with natural ligands to become photothermal materials and also demonstrate the ability to display heavy metals from water (Bassyouni et al 2020; Zhang et al 2019a). The implementation of fish scales as photothermal materials appears to be very significant in seawater desalination technology.

Crystallinity Analysis. Figure 4 shows similar crystallographic characteristics of the XRD diffractograms of the two types of fish scale, termed PF and RS. Consequently, six reflection peaks were associated with an angle of 2θ for the PF, including $25,92^0$, 31.97^0 (maximum intensity), 39.85^0, 46.76^0, 49.54^0 and 53.09^0, while the RS recorded $25,92^0$, 32.07^0 (maximum intensity), 39.46^0, 47.05^0, 49.64^0 and 53.39^0. The profile of the diffraction

peaks indicated lesser fish scale crystals or structural irregularities with low crystallinity (Silva et al 2019). The 2θ angles related to the peaks of the XRD spectra were known to correspond to the hydroxyapatite structure, that is, a crystal with a hexagonal structure (Torres et al 2008; Ikoma et al 2003).

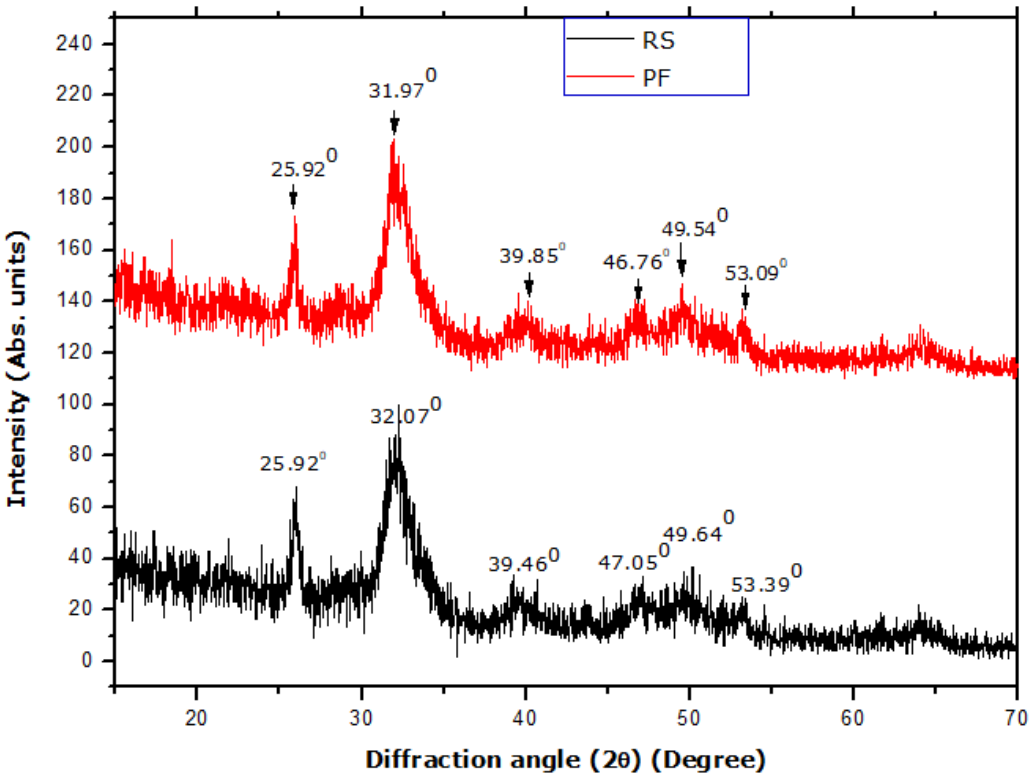

Figure 4. X-ray diffractogram for fish scale samples.
Source: Authors' elaboration

Hydroxyapatite ($Ca_{10}(PO_4)_6(OH)_2$) is a very promising material for the purification of air, water, and soil from contaminated sources (Ibrahim et al 2020). Previous studies used a composite of hydroxyapatite, polydopamine (PDA), and chitosan nanowires as membranes for photothermal effect-driven saltwater distillation (Cao et al 2020). Hydroxyapatite nanowires are superior templates for forming stable, dense, and efficient PDA layers (Cao et al 2020). Nano-hydroxyapatite also served as a natural template for the synthesis of porous carbon materials (Huang et al 2015). CNTs/hydroxyapatite composites have been synthesized (Pei et al 2011). This study confirmed the potential of nano-hydroxyapatite as a template or substrate for the growth of photothermal nanomaterials, including CNTs.

Characteristic morphology. Figures 5a and 5b represent the morphological characteristics of red snapper and parrotfish scale powder after SEM analysis, respectively. The results showed the presence of collagen fibers and hydroxyapatite crystals (Silva et al 2019; Santos et al 2009; Ikoma et al 2003). The SEM image verified the amorphous nature of the fish scales detected by XRD and also observed a regular wavy morphology in the lamellae region similar to the shape of parallel grooves.

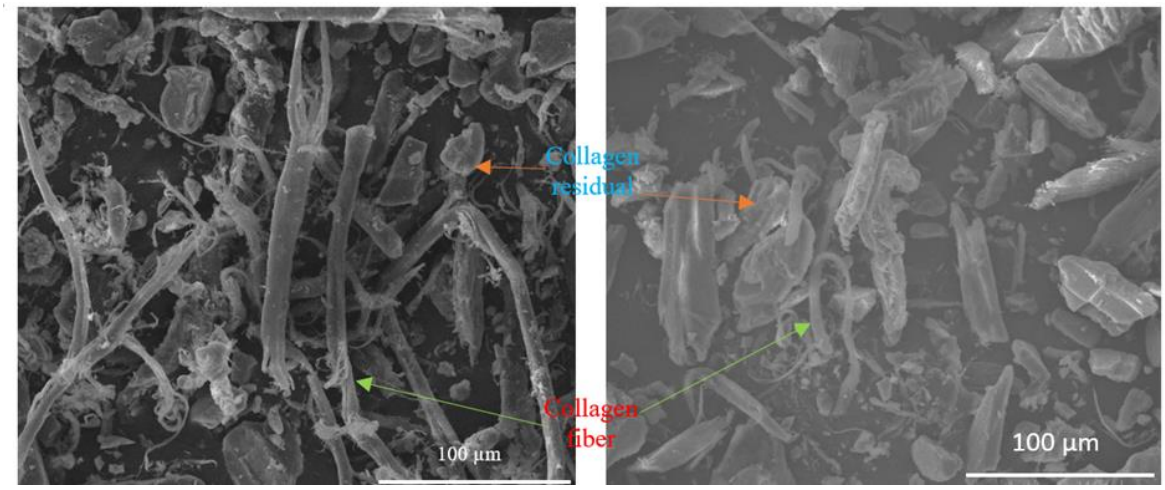

a. RS powder b. PF powder

Figure 5. SEM photo of fish scales.
Source: Photos taken by authors

Figure 6 indicates three different levels of structural characteristics in the fish scale lamellae, commencing from top to bottom: the bone, transition, and matrix layers (Feng et al 2020). Type 1 collagen represents the primary component of the matrix, including a small amount of hydroxyapatite, while the bone and transition layers are composed of randomly oriented collagen fibers (Feng et al 2020). Morphological analysis confirmed that both parrotfish and red snapper powder are made up of collagen and hydroxyapatite. Wastes are possibly applied as raw materials in the manufacture of carbon nanocomposite substances.

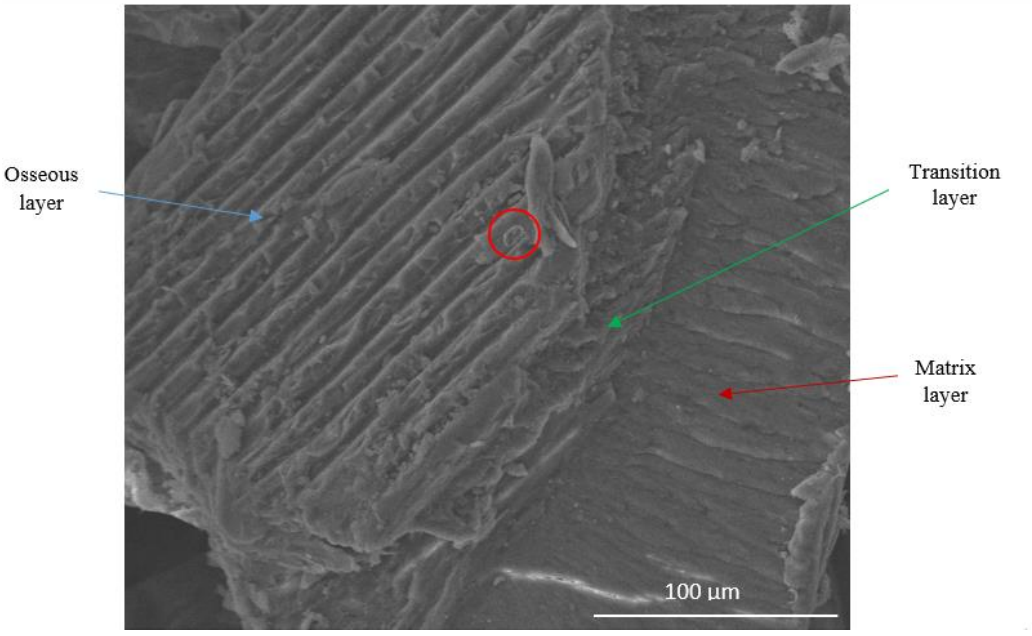

Figure 6. Cross-section of parrotfish scale lamellae.
Source: Photos taken by authors

Conclusions. Studies on chemical composition and bonding, light absorption, crystallinity, as well as the morphology of parrotfish and red snapper scales provided significant recommendations for the application of aquatic biomass as raw materials for photothermal substances. The primary components, including collagen and hydroxyapatite, were the main sources for the manufacture of carbon nanocomposites. Furthermore, iron and calcium content tend to accelerate the pyrolytic process of biomass into carbon

nanocomposites. The presence of carboxyl groups in collagen instigated the photothermal process in a unique transition of π to π*. This technique is possibly optimized when fish scales are converted into one of the allotropes of carbon nanomaterials, including CNTs or CNDs. The wastes are potentially applied in seawater desalination technology.

Acknowledgements. The authors would like to thank the Sam Ratulangi University for the financial support through PNBP Fund, for the fiscal year 2022.

Conflict of interest. The authors declare no conflict of interest.

References

Achieng G. O., Kowenje C. O., Lalah J. O., Ojwach S. O., 2019 Preparation, characterization of fish scales biochar and their applications in the removal of anionic indigo carmine dye from aqueous solutions. Water Science and Technology 80(11):2218–2231.

Ahmadvand S., Abbasi B., Azarfar B., Elhashimi M., Zhang X., Abbasi B., 2019 Looking beyond energy efficiency: An applied review of water desalination technologies and an introduction to capillary-driven desalination. Water 11(4):696.

Arola D., Murcia S., Stossel, M., Pahuja R., Linley T., Devaraj A., Ramulu M., Ossa E. A., Wang J., 2018 The limiting layer of fish scales: structure and properties. Acta Biomaterialia 67: 319–330.

Arykbaev R. K., Efimov V. B., Fursova T. N., Likhter A. M., Rybakov A. V, Semenov I. I., Stefanova G. P., Shishkanova I. A., Varlamova K. S., Vybornov N. A., 2020 Study of Electrical and Optical Properties of Biomaterials Based on Fisch Scales. Journal of Surface Investigation: X-Ray, Synchrotron and Neutron Techniques 14:422–427.

Athinarayanan J., Periasamy V. S., Alshatwi A. A., 2020 Simultaneous fabrication of carbon nanodots and hydroxyapatite nanoparticles from fish scale for biomedical applications. Materials Science and Engineering: C 117:111313.

Bassyouni M., Mansi A. E., Elgabry A., Ibrahim B. A., Kassem O. A., Alhebeshy R., 2020 Utilization of carbon nanotubes in removal of heavy metals from wastewater: A review of the CNTs' potential and current challenges. Applied Physics A 126(1):1–33.

Bunaciu A. A., UdriŞTioiu E. G., Aboul-Enein H. Y., 2015 X-ray diffraction: instrumentation and applications. Critical Reviews in Analytical Chemistry 45(4):289–299.

Cao S., Wu X., Zhu Y., Gupta R., Tan A., Wang Z., Jun Y. S., Singamaneni S., 2020 Polydopamine/hydroxyapatite nanowire-based bilayered membrane for photothermal-driven membrane distillation. Journal of Materials Chemistry A 8(10):5147–5156.

Chen B., Han M. Y., Peng K., Zhou S. L., Shao L., Wu X. F., Wei W. D., Liu S. Y., Li Z., Li J. S., 2018 Global land-water nexus: Agricultural land and freshwater use embodied in worldwide supply chains. Science of the Total Environment 613:931–943.

Chen C., Li Y., Song J., Yang Z., Kuang Y., Hitz E., Jia C., Gong A., Jiang F., Zhu J. Y., 2017 Highly flexible and efficient solar steam generation device. Advanced Materials 29(30):1701756.

Dao V., Choi H., 2018 Carbon-based sunlight absorbers in solar-driven steam generation devices. Global Challenges 2(2):1700094.

Feng H., Li X., Deng X., Li X., Guo J., Ma K., Jiang B., 2020 The lamellar structure and biomimetic properties of a fish scale matrix. RSC Advances 10(2):875–885.

Gao M., Zhu L., Peh C. K., Ho G. W., 2019 Solar absorber material and system designs for photothermal water vaporization towards clean water and energy production. Energy & Environmental Science 12(3):841–864.

Gao Q., 2021 Ultrasonic extraction and identification of carp scale collagen. Journal of Physics: Conference Series 1732(1):12111.

Ghasemi H., Ni G., Marconnet A. M., Loomis J., Yerci S., Miljkovic N., Chen G., 2014 Solar steam generation by heat localization. Nature Communications 5:4449.

Ghods S., Waddell S., Weller E., Renteria C., Jiang H.Y., Janak J. M., Mao S. S., Linley T. J., Arola D., 2020 On the regeneration of fish scales: structure and mechanical behavior. Journal of Experimental Biology 223(10):1-11.

Gueymard C. A., 2004 The sun's total and spectral irradiance for solar energy applications and solar radiation models. Solar Energy 76(4): 423–453.
Han B., Zhang Y., Chen Q., Sun H., 2018 Carbon-Based Photothermal Actuators. Advanced Functional Materials 28(40):802235.
Han X., Wang W., Zuo K., Chen L., Yuan L., Liang J., Li Q., Ajayan P. M., Zhao Y., Lou J., 2019 Bio-derived ultrathin membrane for solar driven water purification. Nano Energy 60:567–575.
Hargreaves J. S. J., 2016 Some considerations related to the use of the Scherrer equation in powder X-ray diffraction as applied to heterogeneous catalysts. Catalysis, Structure & Reactivity 2(1–4):33–37.
He Z., Cheng G., Jiang Y., Li Y., Zhu J., Meng W., Zhou H., Dai L., Wang L., 2020 Novel 2D porous carbon nanosheet derived from biomass: Ultrahigh porosity and excellent performances toward V2+/V3+ redox reaction for vanadium redox flow battery. International Journal of Hydrogen Energy 45(7):3959–3970.
Hou, Q., Xue, C., Li, N., Wang, H., Chang, Q., Liu, H., Yang, J., & Hu, S., 2019. Self-assembly carbon dots for powerful solar water evaporation. Carbon 149:556–563.
Huang B., Shao H., Liu N., Xu Z. J., Huang Y., 2015 From fish scales to highly porous N-doped carbon: a low cost material solution for CO_2 capture. RSC Advances 5(107): 88171–88175.
Ibrahim M., Labaki M., Giraudon J. M., Lamonier J. F., 2020 Hydroxyapatite, a multifunctional material for air, water and soil pollution control: A review. Journal of Hazardous Materials 383:121139.
Ikoma T., Kobayashi H., Tanaka J., Walsh D., Mann S., 2003a Microstructure, mechanical, and biomimetic properties of fish scales from *Pagrus major*. Journal of Structural Biology 142(3):327–333.
Ikoma T., Kobayashi H., Tanaka J., Walsh D., Mann S., 2003b Physical properties of type I collagen extracted from fish scales of *Pagrus major* and *Oreochromis niloticas*. International Journal of Biological Macromolecules 32(3–5):199–204.
Ilnicka A., Lukaszewicz J. P., 2018 Marine and freshwater feedstocks as a precursor for nitrogen-containing carbons: a review. Marine Drugs 16(5):142.
Jafari H., Lista A., Siekapen M. M., Ghaffari-Bohlouli P., Nie L., Alimoradi H., Shavandi A., 2020 Fish Collagen: Extraction, Characterization, and Applications for Biomaterials Engineering. Polymers 12(10):2230.
Jiang F., Liu H., Li Y., Kuang Y., Xu X., Chen C., Huang H., Jia C., Zhao X., Hitz, E., 2018 Lightweight, mesoporous, and highly absorptive all-nanofiber aerogel for efficient solar steam generation. ACS Applied Materials & Interfaces 10(1):1104–1112.
Kabir S. M., Cueto R., Balamurugan S., Romeo L. D., Kuttruff J. T., Marx, B. D., Negulescu I. I., 2019 Removal of acid dyes from textile wastewaters using fish scales by absorption process. Clean Technologies 1(1):311–324.
Li Z., Siddiqi A., Anadon L. D., Narayanamurti V., 2018 Towards sustainability in water-energy nexus: Ocean energy for seawater desalination. Renewable and Sustainable Energy Reviews 82:3833–3847.
Listiaji P., Suparta G. B., 2020 Low-cost imaging spectrophotometer system for absorbance measurement. Journal of Physics: Conference Series 1567(4):42093.
Liu F., Lai Y., Zhao B., Bradley R., Wu W., 2019 Photothermal materials for efficient solar powered steam generation. Frontiers of Chemical Science and Engineering 13:636-653.
Liu Y., Guo N., Yin P., Zhang C., 2019 Facile growth of carbon nanotubes using microwave ovens: the emerging application of highly efficient domestic plasma reactors. Nanoscale Advances 1(12):4546–4559.
Liyanaarachchi S., Shu L., Muthukumaran S., Jegatheesan V., Baskaran K., 2014 Problems in seawater industrial desalination processes and potential sustainable solutions: a review. Reviews in Environmental Science and Bio/Technology 13(2): 203–214.
Luo J., Wan Y., 2013 Effects of pH and salt on nanofiltration—a critical review. Journal of Membrane Science 438:18–28.
Meng W., Bai X., Wang B., Liu Z., Lu S., Yang B., 2019 Biomass-Derived Carbon Dots and Their Applications. Energy & Environmental Materials 2(3):172–192.

Müsellim E., Tahir M. H., Ahmad M. S., Ceylan S., 2018 Thermokinetic and TG/DSC-FTIR study of pea waste biomass pyrolysis. Applied Thermal Engineering 137:54–61.
Ni G., Zandavi S. H., Javid S. M., Boriskina S. V, Cooper T. A., Chen G., 2018 A salt-rejecting floating solar still for low-cost desalination. Energy & Environmental Science 11(6):1510–1519.
Paul S., Pal,A., Choudhury A. R., BodhakS., Balla V. K., Sinha A., Das M., 2017 Effect of trace elements on the sintering effect of fish scale derived hydroxyapatite and its bioactivity. Ceramics International 43(17):15678–15684.
Pei X., Wang J., Wan Q., Kang L., Xiao M., Bao H., 2011 Functionally graded carbon nanotubes/hydroxyapatite composite coating by laser cladding. Surface and Coatings Technology 205(19):4380–4387.
Poblete R., Cortes E., Bakit J., Luna-Galiano Y., 2020 Use of fish scales as an adsorbent of organic matter present in the treatment of landfill leachate. Journal of Chemical Technology & Biotechnology 95(5):1550–1558.
Rahmani K., Jadidian R., Haghtalab, S., 2016 Evaluation of inhibitors and biocides on the corrosion, scaling and biofouling control of carbon steel and copper–nickel alloys in a power plant cooling water system. Desalination 393:174–185.
Rumengan I. F. M., Suptijah P., Wullur S., Talumepa A., 2017 Characterization of chitin extracted from fish scales of marine fish species purchased from local markets in North Sulawesi, Indonesia. IOP Conf. Series: Earth and Environmental Science, 89:1315–1755.
Sahoo S. R., Sri A. G., Mishra, C., 2019 Preparation of activated carbon from fish scale. International Journal of Advance Research and Development 4(4):1-2.
Santana C. A., Andrade L. H. C., Súarez Y. R., Yukimitu K., Moraes J. C. S., Lima, S. M., 2015 Fourier transform-infrared photoacoustic spectroscopy applied in fish scales to access environmental integrity: A case study of Astyanax altiparanae species. Infrared Physics & Technology 72:84–89.
Santos E. de B., Vieira E. F. da S., Cestari A. R., Barreto, L. S., 2009 Characterization of the piau fish (*Leporinus elongatus*) scales and their application to remove Cu (II) from aqueous solutions. Química Nova 32(1):134–138.
Sengupta J., Jacob, C., 2010 The effect of Fe and Ni catalysts on the growth of multiwalled carbon nanotubes using chemical vapor deposition. Journal of Nanoparticle Research 12(2):457–465.
Sharif M. N., Haider H., Farahat A., Hewage K., Sadiq, R., 2019 Water–energy nexus for water distribution systems: a literature review. Environmental Reviews 27(4):519–544.
Silva A. V. S., Torquato L. D. M., Cruz, G., 2019 Potential application of fish scales as feedstock in thermochemical processes for the clean energy generation. Waste Management 100:91–100.
Suo-Lian W., Huai-Bin K., Dong-Jiao, L., 2017 Technology for extracting effective components from fish scale. J Food Sci Eng 7(7):351–358.
Suriani A. B., Asli N. A., Salina M., Mamat M. H., Aziz A. A., Falina A. N., Maryam M., Shamsudin M. S., Nor R. M., Abdullah S., 2013 Effect of iron and cobalt catalysts on the growth of carbon nanotubes from palm oil precursor. IOP Conference Series: Materials Science and Engineering 46(1):12014.
Torres F. G., Troncoso O. P., Nakamatsu J., Grande C. J., Gomez C. M., 2008 Characterization of the nanocomposite laminate structure occurring in fish scales from Arapaima gigas. Materials Science and Engineering C 28(8):1276–1283.
Ullah I., Rasul, M. G., 2019. Recent developments in solar thermal desalination technologies: A review. Energies 12(1):119.
Vélez-Cordero J. R., Hernandez-Cordero J., 2015 Heat generation and conduction in PDMS-carbon nanoparticle membranes irradiated with optical fibers. International Journal of Thermal Sciences 96:12–22.
Wang H., 2018 Low-energy desalination. Nature Nanotechnology 13(4):273–274.
Wang X., Zhu M., Sun Y., Fu W., Gu Q., Zhang C., Zhang Y., Dai Y., Sun, Y., 2016 A New Insight of the Photothermal Effect on the Highly Efficient Visible-Light-Driven Photocatalytic Performance of Novel-Designed TiO2 Rambutan-Like Microspheres

Decorated by Au Nanorods. Particle & Particle Systems Characterization 33(3):140–149.
Wang Z., Horseman T., Straub A. P., Yip N. Y., Li D., Elimelech M., Lin, S., 2019 Pathways and challenges for efficient solar-thermal desalination. Science Advances 5(7):eaax0763.
Wilson H. M., Ar S. R., Jha N., 2020 Plant-derived carbon nanospheres for high efficiency solar-driven steam generation and seawater desalination at low solar intensities. Solar Energy Materials and Solar Cells 210:110489.
Xia Y., Hou Q., Jubaer H., Li Y., Kang Y., Yuan S., Liu H., Woo M. W., Zhang L., Gao, L., 2019 Spatially isolating salt crystallisation from water evaporation for continuous solar steam generation and salt harvesting. Energy & Environmental Science 12(6):1840–1847.
Xu Y., Yin J., Wang J., Wang X., 2019 Design and optimization of solar steam generation system for water purification and energy utilization: A review. Reviews on Advanced Materials Science 58(1): 226–247.
Yadav M., Goswami P., Paritosh K., Kumar M., Pareek N., Vivekanand V., 2019 Seafood waste: a source for preparation of commercially employable chitin/chitosan materials. Bioresources and Bioprocessing 6(1):8.
Yang R., Liu S., Liu Y., Liu L., Chen L., Yu W., Yan Y., Feng Z., Xu Y., 2021 Decalcified fish scale-based sponge-like nitrogen-doped porous carbon for lithium-sulfur batteries. Ionics(27): 165–174.
Yin Z., Wang H., Jian M., Li Y., Xia K., Zhang M., Wang C., Wang Q., Ma M., Zheng Q., 2017 Extremely black vertically aligned carbon nanotube arrays for solar steam generation. ACS Applied Materials & Interfaces 9(34):28596–28603.
Yu J. G., Zhao X. H., Yu L. Y., Jiao F. P., Jiang J. H., Chen X. Q., 2014 Removal, recovery and enrichment of metals from aqueous solutions using carbon nanotubes. Journal of Radioanalytical and Nuclear Chemistry 299(3):1155–1163.
Yuan R., Yu S., Shen Y., 2019 Pyrolysis and combustion kinetics of lignocellulosic biomass pellets with calcium-rich wastes from agro-forestry residues. Waste Management 87:86–96.
Zhang C., Liang H., Xu Z., Wang Z., 2019a Harnessing Solar-Driven Photothermal Effect toward the Water–Energy Nexus. Advanced Science 6(18):1900883.
Zhang L., Chen L., Liu J., Fang X., Zhang Z., 2016 Effect of morphology of carbon nanomaterials on thermo-physical characteristics, optical properties and photo-thermal conversion performance of nanofluids. Renewable Energy 99:888–897.
Zhang Q., Xu W., Wang X., 2018 Carbon nanocomposites with high photothermal conversion efficiency. Science China Materials 61(7):905–914.
Zhang Y., Gao Z., Yang X., Chang J., Liu Z., Jiang K., 2019b Fish-scale-derived carbon dots as efficient fluorescent nanoprobes for detection of ferric ions. RSC Advances 9(2):940–949.

Received: 09 Septemberr 2021. Accepted: 29 June 2022. Published online: 06 July 2022.
Authors:
Dolfie P. Pandara, Physics Study Program, Faculty of Mathematics and Science, Sam Ratulangi University, Kampus Bahu St., 95115 Manado, North Sulawesi, Indonesia, e-mail: dpandara_fisika@unsrat.ac.id
Kawilarang W. A. Masengi, Marine Science Doctoral Study Program, Faculty of Fisheries and Marine Science, Sam Ratulangi University, Kampus Bahu St., 95115 Manado, North Sulawesi, Indonesia, e-mail: alex_masengi@unsrat.ac.id
Gerald H. Tamuntuan, Physics Study Program, Faculty of Mathematics and Science, Sam Ratulangi University, Kampus Bahu St., 95115 Manado, North Sulawesi, Indonesia, e-mail: gtamuntuan@gmail.com
Ping A. Angmalisang, Marine Science Doctoral Study Program, Faculty of Fisheries and Marine Science, Sam Ratulangi University, Kampus Bahu St., 95115 Manado, North Sulawesi, Indonesia, e-mail: astoni_angmalisang@unsrat.ac.id
Audy D. Wuntu, Chemistry Study Program, Faculty of Mathematics and Science, Sam Ratulangi University, Kampus Bahu St., 95115 Manado, North Sulawesi, Indonesia, e-mail: wuntudenny@unsrat.ac.id
Ferdy Ferdy, Physics Study Program, Faculty of Mathematics and Science, Sam Ratulangi University, Kampus Bahu St., 95115 Manado, North Sulawesi, Indonesia, e-mail: ferdysagita19@gmail.com
Maria D. Bobanto, Physics Study Program, Faculty of Mathematics and Science, Sam Ratulangi University, Kampus Bahu St., 95115 Manado, North Sulawesi, Indonesia, e-mail: mariabobanto5@unsrat.ac.id
Armstrong F. Sompotan, Physics Study Program, Faculty of Mathematics and Science, Manado State University, Kampus Unima St., 95618 Tondano, North Sulawesi, Indonesia, e-mail: armstrong@unima.ac.id

How to cite this article:
Pandara D. P., Masengi K. W. A., Tamuntuan, G. H., Angmalisang P. A., Wuntu A. D., Ferdy F., Bobanto M. D., Sompotan A. F., 2022 The potential of fish scale application as photothermal raw material in seawater desalination. AACL Bioflux 15(4):1617-1629.